(This is a sample cover image for this issue. The actual cover is not yet available at this time.)

Composites: Part A 46 (2013) 147–153

Contents lists available at SciVerse ScienceDirect

Composites: Part A

journal homepage: www.elsevier.com/locate/compositesa

Multiscale hybrid atomistic-FE approach for the nonlinear tensile behaviour of graphene nanocomposites

Y. Chandra [a], F. Scarpa [b], R. Chowdhury [c], S. Adhikari [a,*], J. Sienz [a]

[a] Swansea University, Swansea SA2 8PP, UK
[b] Advanced Composites Centre for Innovation and Science, University of Bristol, Bristol BS8 1TR, UK
[c] Department of Civil Engineering, Indian Institute of Technology Roorkee, Roorkee 247 667, India

ARTICLE INFO

Article history:
Received 13 August 2012
Received in revised form 28 October 2012
Accepted 13 November 2012
Available online 29 November 2012

Keywords:
A. Nano-structures
B. Delamination
B. Fracture toughness
C. Finite element analysis (FEA)

ABSTRACT

The paper introduces a multiscale modelling approach to simulate the nonlinear tensile behaviour of nancomposites with single layer graphene (SLG) reinforcement. The graphene nanoinclusions are represented at the nanoscale through an atomistic Finite Element model and the matrix material is approximated by continuum 3D elements. Two different configurations of SLG composites have been studied based on a continuous and short type of reinforcements. The effect of the orientation of graphene sheet on the stiffness of the composite structure has also been evaluated. The multiscale model presented in this work is able to predict features such as debonding, nonlinearity in polymer and strain based damage criteria for the matrix. Stiffness and strength values computed with this model compare well with experimental results available in open literature.

1. Introduction

Graphene sheets are considered to be the thinnest, strongest and stiffest materials produced by mankind [1–4]. Earliest work on these carbon-based materials can be traced back to 1960s [5,6]. However, only during the last decade few-layers of graphitic planes nanostructures have been produced and characterised [7]. Single and few-layers graphene sheets offer enhanced mechanical [8–17] and electrical [18–22,21,23,24] properties compared to other types of reinforcement at nanoscale, such as carbon-based nanotubes. Various manufacturing routes are available to extract graphene sheets, including thermal exfoliation [25,26], epitaxial heat treatment of silicon carbide (SiC) [27,28] and also by cutting open carbon nano tubes (CNTs) [19]. In composite materials, carbon based nanostructures such as graphene and carbon nano tubes (CNTs) can be either used as long fibre-type reinforcements, or nanoinclusions. Graphene-based reinforcements pose various advantages over conventional fibres such as carbon, glass, and aramid fibres in terms of strength and stiffness, decreased weight and enhanced electrical properties. The exceptional scale of electrical conductivity [18] displayed by these thin carbon films embedded in polymer matrix make them a suitable candidate in aerospace applications for electromagnetic compatibility. As per the review conducted by Hussain et al. [29], there is a growing market demand for nanocomposites, although the authors have pointed out various issues, such as the inability to attain strong bonding between matrix and reinforcement, the difficulty in dispersing the nanoparticles in the matrix, and reinforcement alignment issues. It is therefore necessary to consider these aspects at the simulation stage, to provide the composite designer predicting tools with sufficient fidelity. The computational modelling of the mechanical properties related to graphene sheets at atomic scale has been presented by many authors [8–10,14,17,49,50,57]. Atomistic Finite Element modelling applied to carbon nanosheets by employing Morse and Amber force field constants has been presented by Scarpa et al. [8,9,15,16]. Similar modelling techniques have also been used by Pour et al. [10,30]. The Authors have recently developed a numerical model for graphene sheets, in which equivalent homogenised properties of C–C bonds of the graphene lattice are expressed in terms of thickness, equilibrium lengths and force-field models [8]. The covalent bonds between a pair of carbon atoms are modelled by deep shear Timoshenko beams with stretching, bending, torsional and deep shear deformation. The properties of these deep shear beams are derived based on the equivalence between the harmonic potential. The force constants of this harmonic potential can be either based on the Morse model or the Amber model [31]. The geometric configurations and mechanical properties are represented as truss assemblies (Finite Elements), for which the total potential energy associated to the loading is calculated. The final thickness and average equilibrium lengths of the bonds correspond to the minimum potential energy configuration of the nanostructure.

* Corresponding author. Tel.: +44 (0)1792 602088; fax: + 44 (0)1792 295676.
E-mail address: S.Adhikari@swansea.ac.uk (S. Adhikari).

1359-835X/$ - see front matter © 2012 Elsevier Ltd. All rights reserved.
http://dx.doi.org/10.1016/j.compositesa.2012.11.006

Nanocomposites based on graphene reinforcement can be considered as two or multiphase materials, represented at their most basic configuration by the presence of a nanoinclusion and a surrounding matrix. At meso and nanoscale, the polymer matrix can be considered as forming a continuous structure. The structural response of the continuum matrix implies a mechanical modelling at microscale. However, graphene sheets can be numerically represented by an array of hexagonally oriented beam elements. These beams represent the sp^2 covalent bonds, while nodes of the same elements represent carbon atoms. Numerically, the polymer matrix at microscale can be approximated by 3D solid hexahedral elements. In physical reality the polymer matrix is connected to graphene sheets through weak van der Waals forces, when no functional groups exist. These van der Waals forces can be represented by LJ (Lennard–Jones) potential forces. Numerically, the LJ potential attractive and repulsive forces between the fibre and the matrix can be transferred through spring elements.

This work describes a multiscale approach to simulate the tensile properties of graphene-reinforced nanocomposites. At macroscale level, the polymer matrix is represented by 3D continuum elements with three translational and three rotational degrees of freedom to the polymer structure. The weak bonding between the matrix and the fibre is modelled with the aid of LJ potential theory, where bonds are represented by nonlinear springs. The graphene sheet is represented at atomic (i.e. nano) scale and using an atomistic-FE model based on beams with stretching, bending, deep shear and torsional capabilities, also in the nonlinear geometric displacement regime. The finite element model of the graphene sheet reinforced polymer (GSRP) is depicted in Fig. 1. The impact of different geometrical configurations (armchair and zigzag orientations), boundary conditions and aspect ratio on the GSRP are investigated in the present study. We propose also an analytical plate model to simulate in a compact form the mechanical behaviour of GSRP, providing a further benchmark to the multiscale finite element (FE) model of the GSRP. The FE code ABAQUS™ 6.10 [38] has been used for its capability to incorporate damage laws in composites and its use of Python language scripts and subroutines to simulate the debonding at the interface.

The model used in this work describes the graphene system with an FE atomistic model represented by higher order Timoshenko beam elements, contrary to the majority of FE-based atomistic representations of sp^2 C–C bonds made with Euler–Bernoulli beams [10,13,14,30,50]. Euler–Bernoulli and Timoshenko beams provide correct deformation mechanisms when the same force model used [53]. However different sets of thickness for the beams must be adopted, the Timoshenko ones provide values closer to the ones identified by Molecular Dynamics or DFT simulations [16,35]. The originality of the present model lies in its closeness to experimental results with realistic weight fraction values (0.05–1.5%) [42,43,45,47,48], with the present work focusing on 0.05 wt.%. Another original feature of the model presented in this work is its ability to capture the overall nonlinear behaviour of the composite and the failure mechanism of the polymer matrix. Recently, Prashar et al. [49] have studied buckling behavior of the epoxy resin reinforced with graphene and reported enhancement of buckling strength by 26% due to the reinforcement. Montazeri et al. [50] have computed the linear elastic modulus of graphene reinforced polymers by considering thermally produced ripples and sliding motion in the graphene sheet. Tserpes et al. [51] produced an RVE (representative volume element) of CNT reinforced polymer, using a two step approach. The first step consisted of a CNT modelled using a modified Morse potential, to establish the fracture

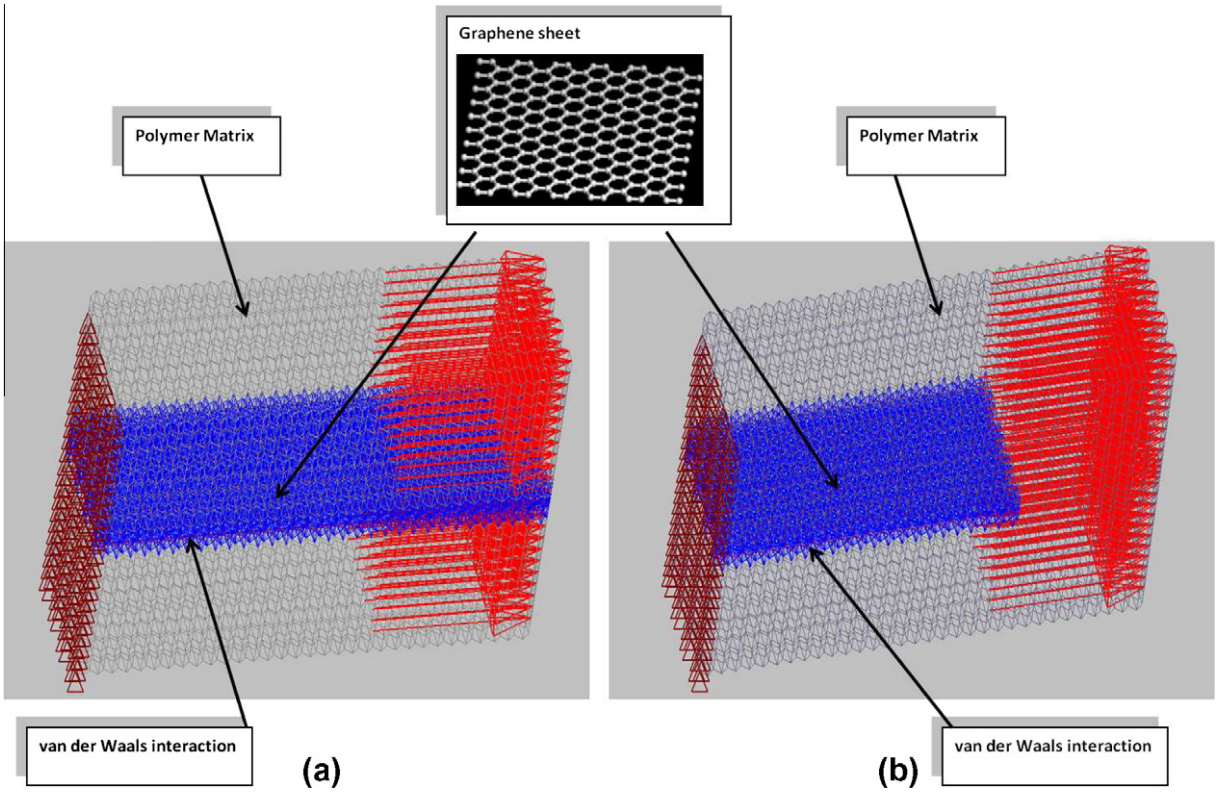

Fig. 1. Multiscale model of GSRP: carbon atoms are represented by nodes, covalent bonds are modelled as Timoshenko beams, LJ potential is modelled by spring elements and the polymer matrix is formed by 3D solid elements. (a) Continuous fibre and (b) short fibre. The two can be taken as representative volume elements (RVEs). The boundary conditions are also shown: the left hand side of the nanocomposite is constrained and the right hand side is loaded. (For interpretation of the references to color in this figure legend, the reader is referred to the web version of this article.)

behaviour of the carbon nanotube. In the second step, a continuous beam with the fracture behaviour of the atomistic CNT was inserted in the composite RVE for the multiscale analysis. Wernik et al. [52] developed a non-linear RVE of CNT reinforced polymers and concluded a considerable enhancement in the stiffness of the polymer. Equivalent numerical approaches have also been used by Li et al. and Shokrieh et al. to describe the mechanical response of epoxy/SWCNT (single wall carbon nanotube) composites [32,33]. However, none of these previous works considered realistic weight fractions of nanostructures and damage mechanisms present in the polymer.

2. Multiscale model of the composite structure

Similar to earlier computational work on graphene sheets [8,9], the sp^2 covalent bonds are represented by deep shear Timoshenko beams with three translation and three rotational degrees of freedom with shear correction. The element type B31 from the ABAQUS™ version 6.10 element library [38] has been employed to simulate covalent bonds. The length of each beam is 0.142 nm (the equilibrium length of C–C sp^2) and the diameter is 0.089 nm [8]. The properties of the beams accounting for the C–C bonds, are calculated based upon the force constants of the covalent bonds given below [8]:

$$\frac{k_r}{2}(\delta r)^2 = \frac{EA}{2L}(\delta r)^2 \tag{1}$$

$$\frac{k_\tau}{2}(\delta \varphi)^2 = \frac{GJ}{2L}(\delta \varphi)^2 \tag{2}$$

$$\frac{k_\theta}{2}(\delta \theta)^2 = \frac{EI}{2L}\frac{4+\Phi}{1+\Phi}(\delta \theta)^2 \tag{3}$$

In the above three equations, k_r represents the stretching force constant, k_τ the out-of-plane torsional constant. The term k_θ represents combined in-plane rotation (bending and torsion), consistent with the harmonic potential approach [8]. The term Φ is the shear correction factor, which becomes significant if the aspect ratio of the beams is lower than 10 [34]. The numerical values of the constants mentioned in the above equations can either be obtained by Morse or Amber models [8]. According to the Morse model, the values of force constants are $k_r = 8.74 \times 10^{-7}$ N mm^{-1}, $k_\theta = 9.00 \times 10^{-10}$ N nm rad^{-2} and $k_\tau = 2.78 \times 10^{-10}$ N nm^{-1} rad^{-2}. For comprehensive understanding of this methodology, readers are referred to [8,15,35]. Table 1 shows the the equivalent material and element property information. In the present work the nonlinearity in covalent bonds has been ignored. The equivalent stress–strain curve for sp^2 C–C covalent bonds and graphene/carbon nanotubes can be found in various works [53–57]. The single C–C bond shows a linear regime under tensile loading up to ~10% [53]. Armchair and zigzag graphene sheets in graphitic state show a substantial linearity of the tensile response up to 10% in Molecular Dynamics models using AIREBO potential [58]. Furthermore, in a nanocomposite with low loading (0.05 wt.% fraction), one can expect larger strain levels occurring in the polymer but not in the graphene sheet. Since the maximum tensile deformation in the present simulations corresponds to 10% of strain, the assumption of linear elastic regime with nonlinear geometric deformation for the graphene can be considered justified.

Similar to the attractive and repulsive forces between layers of graphene sheets in the case of multi layer graphene sheets [9], the graphene sheets are linked to the polymer matrix by van der Waals forces. These van der Waals forces can be mathematically represented by:

$$F_{ij} = \frac{\partial V_{ij}}{\partial r} \tag{4}$$

where r is the atomic displacement along ij (fibre–matrix length). As per Girifalco et al. [36], the force between the atoms (ij) can also be represented by

$$F_{ij} = -12\,\epsilon\left[\left(\frac{r_{min}}{y}\right)^{13} - \left(\frac{r_{min}}{y}\right)^{7}\right] \tag{5}$$

where $y = r_{min} + \delta r$, δr is the atomic displacement along the length ij. The r_{min} (in) is given by $2^{\frac{1}{6}}\sigma$, where $\sigma = (A/B)^{1/6}$. The B and A are attractive and repulsive constants, the values of these constants depend the boundary conditions. In this work we adopt the values for carbon–carbon interaction given in [33,36,37], being equal to 3.4×10^{-4} eV × Å^{12} and 5×10^{-7} eV × Å^6 respectively. The term ϵ is $B^2/(4A)$. In the multiscale models we use nonlinear spring elements to simulate the interaction between reinforcement, with a equivalent force deflection curve calculated using the Eq. (5).

The polymer matrix has been discretized by 3D continuum elements with six degrees of freedom. The type of element used in the ABAQUS™ version 6.10 solver is C3D8I [38]. Isotropic material properties have been assumed to represent the material behaviour of a epoxy matrix. The values of Young's modulus and Poisson's ratio are 2.0 GPa and 0.3 respectively [39]. The nonlinearity in the mechanical behaviour of the polymer matrix has been considered using a Ramberg Osgood approximation [39]. Points of the epoxy stress–strain curve are shown in Table 2.

The FE model with the largest length (8.5 nm) consisted of 1318 beam elements (representing CC bonds), 21,612 spring elements (representing van der Waals interactions) and 64,160 solid elements (representing resin). The nonlinear force–deflection curves both in tension and compression are derived from Eq. (5). The stress and strain data has been collected by constraining one end of the nanocomposite structure, by applying a load to the other end, and by increasing the magnitude of that load until the composite is subjected to tensile strain beyond 9%. Specific models have been developed with the graphene sheet oriented in the space, and for the case of long and short inclusion. While the short inclusion model represents effectively the dispersion of a nanoinclusion in a matrix, the long-type of inclusion (filling the whole length of the RVE) tends to simulate a theoretical nanocomposite with long fibre reinforcement and periodic boundary conditions. A nonlinear Newton–Raphson solver with switch on large deformation effects has been used to simulate the tensile loading [38].

Table 1
Material and element properties for the beam elements used to represent CC bonds. In the table, d is diameter, l is length, A is cross sectional area, E is Young's modulus, v is Poisson's ratio and Φ is the shear correction factor.

Property	Value used in the simulation
d	0.089 nm
l	0.142 nm
A	0.0062 nm^2
E	19.5 GPa
v	0.23
Φ	0.37

Table 2
Points of the stress–strain curve for epoxy matrix based on Ramberg Osgood approximation [39].

Stress (MPa)	Strain (%)
15	1.0
40	2.0
60	3.0
62	4.0

3. Results and discussions

The stress strain curves for two different orientations and for the long and short reinforcement composites are presented in Figs. 2 and 3. For each plot, the stress strain curve has been obtained for three different lengths of the graphene fibre (i.e. 2.7 nm, 5.8 nm and 8.5 nm), corresponding to 0.05 wt.%. The stress has been calculated by straining the material up to 9%. During the simulation it is essential to deactivate the interface bonds if the deflection developed is higher than the cut-off distance 0.85 nm [33]. It is also necessary to generate new bonds if a displaced carbon atom comes in contact with another atom of the matrix. Within the FE code ABAQUS™ version 6.10, this operation is performed by using the commands *Restart and *Modelchange [38]. The nodal displacements in the spring elements (interface bonds) are recorded at each incremental step of the nonlinear loading. If the nodal displacement is found to be beyond the cutoff distance, the analysis is stopped and restarted with an updated position of the nodes belonging to the spring elements. Another *Restart* command is then issued to restart the run from the same increment. Activation and de-activation of the sping element sets are performed using the commands *Modelchange, Remove and *Modelchange, Add. For the type of epoxy material used in this work, one can observe that damage in the polymer has been initiated at 5% plastic strain. At a given strain, the stress developed in the continuous fibre composite is found to be 10 times higher than that of the short fibre composite on average, since the applied load is equally taken by both the reinforcement and the matrix. These plots also contain stresses calculated employing the classical rule of mixture. The analytical values of stresses in the plots, have been calculated using the Young's modulus obtained from the rule of mixtures given in the equations below:

$$E_c = V_f E_f + V_m E_m \tag{6}$$

For the short inclusion composite the relation used to calculate the elastic modulus is [40]:

$$E_s = V_f E_f + \left(1 - \frac{tanh(ns)}{ns}\right) + (1 - V_f)E_f \tag{7}$$

In the above relations, E_c is the elastic modulus of the continuous fibre composite, E_s is the elastic modulus of the short fibre composite, E_f is the elastic modulus of the fibre, E_m is the elastic modulus of the matrix, V_f is the volume fraction of the fibre, V_m is the volume fraction of the matrix, s is L/D, L being the length of the fibre and D being the thickness of the fibre and n is given by:

$$n = \left(\frac{2E_m}{E_f(1+V_m)ln(1/V_f)}\right)^{1/2} \tag{8}$$

From Figs. 2 and 3 it can be observed that the length of the short-type graphene reinforcement does contribute to the overall tensile behaviour of the composite, with the highest global stiffness associated to the nanocomposite with the longest reinforcement. At a given strain, the composite with the long graphene sheet shows stress levels 2% greater than the ones belonging to the short graphene inclusion system. Nonlinearity of the tensile behaviour is however observed also for all the short inclusions lengths around 2% of strain, while the matrix tensile behaviour departs from linearity only from 1% (see Table 2). For the case of continuous graphene reinforcement, the nanocomposite stiffness changes once the stress reaches nonlinearity for strains around 7.5%, independently of the length of the reinforcement in the RVE used. For the long-type graphene reinforcement, higher resistance is carried by the graphene, and a more linear elastic regime is observed because the SLG offers an elastic response to the applied tensile strain up to 25% [41]. At lower strains (below 2%), good agreement is reached between the results from the multiscale model and the rule of mixture predictions.

For the case of continuous graphene reinforcement, the tensile response is found to be stiffer at an orientation angle of 45° because of the arrangement and alignment of C–C covalent bonds in the graphene at graphitic state. The modulus of the composite with the sheet at 0° is 12.8 GPa, while the nanocomposite with a reinforcement at 45° is equal to 17.7 GPa, with a resulting 38% increase in stiffness. The stress strain response is found to be independent of the orientation in the case of short-type reinforcement. At lower strains and under linear elastic regime, the stiffness obtained from the multiscale models are displaying closer correlation with the rule of mixture. For the case of short graphene oriented parallel to the loading direction the stress reaches a maximum value of 77 MPa, but then it decreases with further strain. The maximum stress value for the case of 45° short graphene inclusion orientation is 75 MPa, which represents a 10% strength enhancement compared to the baseline epoxy [39]. This enhancement in strength is found to be comparable with the work of other authors (refer Table 3), in particular with experimental

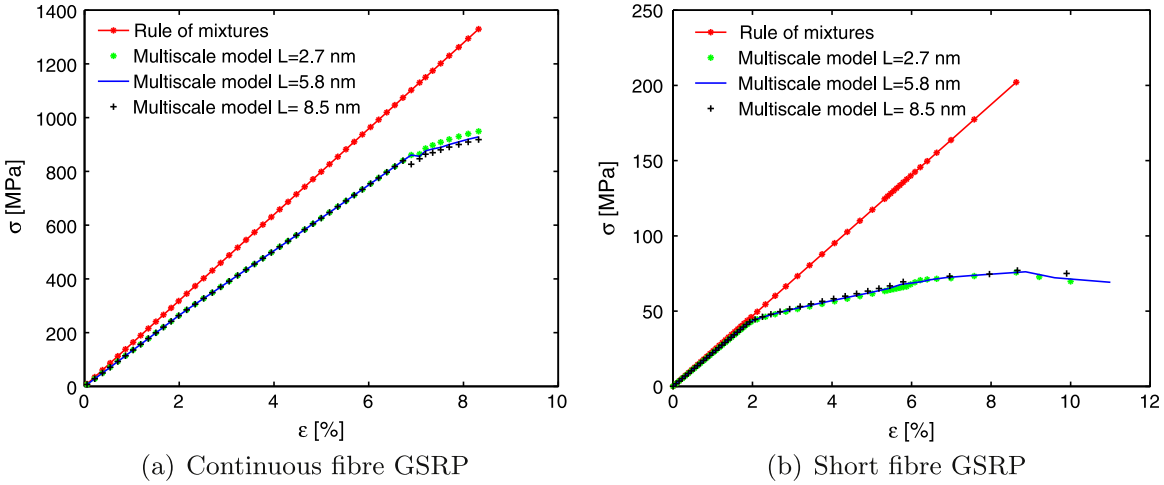

(a) Continuous fibre GSRP (b) Short fibre GSRP

Fig. 2. Variation of stress against strain in the graphene based composite material. Numerically computed stress values are compared against those of computed by analytical rule of mixture theory. The orientation of fibre considered is parallel to the axis of load application. The curve drops at 77 MPa indicating an ultimate tensile strength for short fibre GSRP. (For interpretation of the references to color in this figure legend, the reader is referred to the web version of this article.)

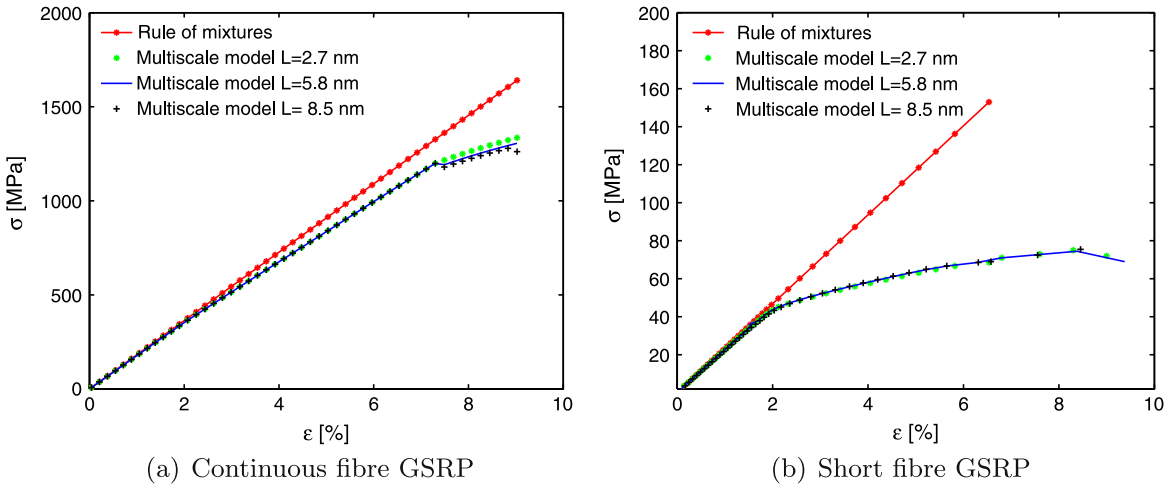

Fig. 3. Variation of stress–strain curves in SLG-based composites. The FE-derived stress values are compared against those from the rule of mixture. The orientation of reinforcement is 45° with respect to the axis of load application. Failure strength for the short fibre GSRP is observed at 75 MPa at 8.5% of strain. (For interpretation of the references to color in this figure legend, the reader is referred to the web version of this article.)

Table 3
Experimental stiffness and strength enhancements in graphene-based polymers (epoxy matrix) from open literature. TRG stands for thermally reduced graphene sheets, GO is graphene oxide, MLGS is multi layer graphene sheets, GNP is graphite nanoplatelets and SLGS is single layer graphene sheet.

Authors	Graphene type	Concentration of graphene (wt.%)	Stiffness enhancement	Strength enhancement
Rafiee et al. [42,43]	FGS	0.05%	10.7%	10.3%
Liu et al. [45]	GO	0.05%	2% (Flexural)	9% (Flexural)
Li et al. [46]	MLGS	N/A	33.33%	36.5%
Cho et al. [47]	GNP	1%	16%	N/A
Ramanathan et al. [48]	FGS	1%	1.8%	1.3%
Present work	SLGS	0.05%	12.5%	10.1%

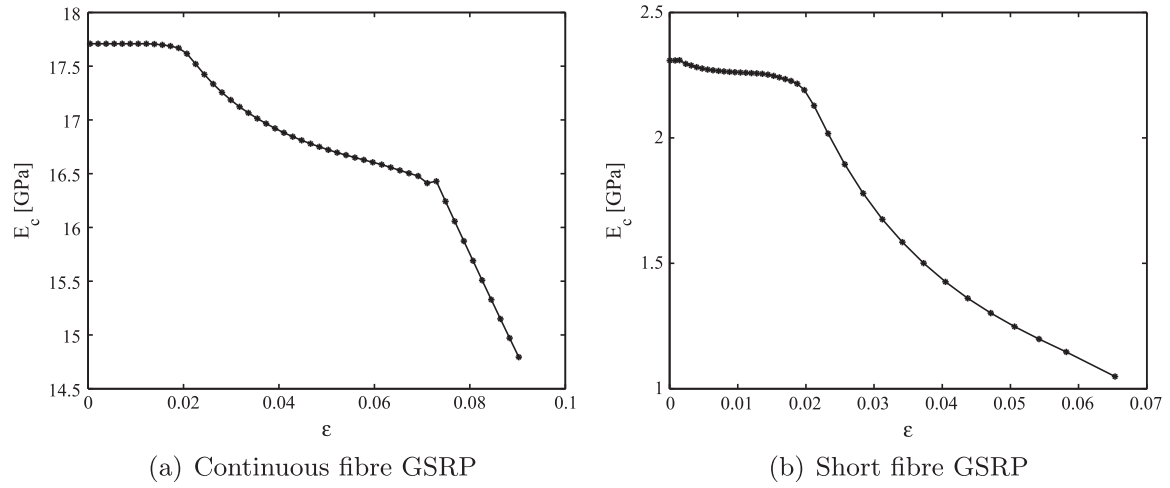

Fig. 4. Variation of secant modulus with strain. The orientation of the fibre is parallel to the axis of the load application.

findings from functionalised graphene sheets (FGSs) dispersed in epoxy matrix by Rafiee et. al. [42,43].

The secant modulus of the continuous graphene reinforced composite (Fig. 4) is close to 17.7 GPa in the linear regime (i.e., equal to the Young's modulus), being 8.85 times higher than the one of the matrix alone. At higher strains (beyond 2%), the secant modulus decreases with strain, indicating a global softening effect. Due to the damage of the LJ bonds, the modulus suddenly decreases and then displays a small increase due to the progressive attachment of bonds with carbon atoms. During the final stage of the tensile loading, the modulus drops continuously as the stress strain response of the polymer becomes more nonlinear. The modulus of the short graphene composite is close to 2.25 GPa at lower strains, with a resulting increase of stiffness by 12.5% over the baseline matrix due to the inclusion of the graphene filler. Similar increase in stiffness has been reported by other authors [42–44] (see Table 3). At higher strains, the modulus decreases continuously due to large geometric deformation and nonlinearity effects in the polymer, as well as de-bonding between reinforcement and matrix due to the failure of the van der Waals interactions.

4. Conclusion

A numerical multiscale approach has been proposed to simulate the nonlinear tensile behaviour of single layer graphene-based composites. The multiscale model includes the representation of inter-atomic covalent C–C sp^2 bonds for the graphene in graphitic (planar) state, and inter matrix-inclusion weak van der Waals forces through LJ potential. Debonding between the matrix and graphene has been represented through activation/deactivation of the nonlinear springs simulating the van der Waals interaction after a cut-off distance (0.85 nm). The model also features the automatic generation of LJ interactions when carbon atoms belonging to strained covalent bonds come into contact with nodes belonging to solid elements of the matrix. In addition, nonlinear geometric large displacements and strain-based failure criteria for the matrix have been applied. The model has been benchmarked for a nanocomposite configuration with 0.05 wt.% against rule of mixture and experimental results available in open literature.

For a constant wt.%, the stress–strain curves obtained do not show a considerable dependence of the results on the length of the graphene reinforcement. This is a clear sign that no evident local scale effects do happen in the numerical representative elementary volume (RVE) used. The results in terms of stiffness and strength for short graphene-type inclusions compare very well with experimental data existing in the open literature. The case for a long-type graphene reinforcement has also been discussed, showing a significant increase both in terms of Young's modulus and linearity of the tensile response compared to the short graphene inclusion case. The orientation of the graphene inclusion is also a factor contributing to the overall mechanical response of the nanocomposite, in particular for the long-type reinforcement where a change in fibre orientation from 0° to 45° with respect to the loading direction provides an increase in the stiffness by 38%. The multiscale model can be used as an effective predicting tool to evaluate graphene nanosystems with different types of matrix and loading conditions. The method presented in this paper can be used for the analysis and design of future generation of graphene composites in a rigours and computationally efficient manner.

Acknowledgements

SA gratefully acknowledges the support of The Royal Society of London through the Wolfson Research Merit award. FS acknowledges the partial support of the European Project FP7-NMP-2009-LARGE-3 M-RECT. JS gratefully acknowledges the support from A4B and WEFO through the WCC and ASTUTE projects.

References

[1] Geim AK, Novoselov KS. The rise of graphene. Nat Mater 2007;6:183–90.
[2] Geim AK. Graphene: status and prospects. Science 2009;324(5934):1530–4.
[3] Novoselov KS. Beyond the wonder material. Phys World 2009;22(8):27–30.
[4] Geim AK. Carbon wonderland. Sci Am 2008;298:90–7.
[5] Boehm H, Clauss A, Fischer G, Hofmann U. Das Adsorptionsverhalten sehr duenner Kohlenstoff-folien. Z Anorg Allg Chem 1962;316(3-4):119.
[6] Boehm H, Clauss A, Fischer G, Hofmann U. Das Adsorptionsverhalten sehr duenner Kohlenstoff-folien. In: Proc. of the fifth conference on carbon. London: Pergamon Press; 1962. p. 73.
[7] Gan Y, Chu W, Qiao L. STM investigation on interaction between superstructure and grain boundary in graphite. Surf Sci 2003;539(1-3):120–8.
[8] Scarpa F, Adhikari S, Phani A. Effective elastic mechanical properties of single graphene sheets. Nanotechnology 2009;20:065709:1–065709:11.
[9] Chandra Y, Chowdhury R, Scarpa F, Adhikari S. Vibrational characteristics of bilayer graphene sheets. Thin Solid Films 2011;519(18):60266032.
[10] Sakhaee-Pour A, Ahmadian MT, Naghdabadi R. Vibrational analysis of single-layered graphene sheets. Nanotechnology 2008;19(8):085702:1.
[11] Chowdhury R, Adhikari S, Scarpa F, Friswell MI. Transverse vibration of single layer graphene sheets. J Phys D: Appl Phys 2011;44(20):205401:1–205401:11.
[12] Gupta SS, Batra RC. Elastic properties and frequencies of free vibrations of single-layer graphene sheets. J Comput Theor Nanosci 2010;7:1546.
[13] Tserpes KI, Papanikos P. Finite element modeling of single-walled carbon nanotubes. Composites Part B 2005;36:1359.
[14] Shokrieh Mahmood M, Rafiee Roham. Prediction of young's modulus of grpahene sheets and carbon nanotubes using nanoscale continuum mechanics approach. Mater Des 2010;31:790–5.
[15] Scarpa F, Adhikari S. A mechanical equivalence for the poisson's ratio and thickness of C–C bonds in single wall carbon nanotubes. J Phys D: Appl Phys 2008;41(085306):1–5.
[16] Scarpa F, Adhikari S, Gil AJ, Remillat C. The bending of single layer graphene sheets: lattice versus continuum approach. Nanotechnology 2010;20(12):085405.
[17] Sadeghi M, Naghdabadi R. Nonlinear vibrational analysis of single-layer graphene sheets. Nanotechnology 2010;21(10):105705:1–105705:10.
[18] Novoselov K, Geim A, Morozov S, Jiang D, Zhang Y, Dubonos S, et al. Electric field effect in atomically thin carbon films. Science 2004;306(5696):666–9.
[19] Zhang Z, Sun Z, Yao J, Kosynkin DV, Tour JM. Transforming carbon nanotube devices into nanoribbon devices. J Am Chem Soc 2009;131(37):13460–3.
[20] Wang T, Chen G, Wu C, Wu D. Study on the graphite nanosheets/resin shielding coatings. Prog Org Coat 2007;59(2):101–5.
[21] Liang J, Xu Y, Huang Y, Zhang L, Wang Y, Ma Y, et al. Infrared-triggered actuators from graphene-based nanocomposites. J Phys Chem C 2009;113(22):9921–7.
[22] Zhang H-B, Zheng W-G, Yan Q, Yang Y, Wang J-W, Lu Z-H, et al. Electrically conductive polyethylene terephthalate/graphene nanocomposites prepared by melt compounding. Polymer 2010;51(5):1191–6.
[23] Dimitrakopoulos C, Lin Y-M, Grill A, Farmer DB, Freitag M, Sun Y, et al. Wafer-scale epitaxial graphene growth on the si-face of hexagonal sic (0001) for high frequency transistors. J Vac Sci Technol B: Microelectron Nanometer Struct 2010;28(5):985–92.
[24] Lin YM, Dimitrakopoulos C, Jenkins KA, Farmer DB, Chiu HY, Grill A, et al. 100-GHz transistors from wafer-scale epitaxial graphene. Science 2010;327(5966):662.
[25] Schniepp H, Li J, McAllister M, Sai H, Herrera-Alonso M, Adamson D, et al. Functionalized single graphene sheets derived from splitting graphite oxide. J Phys Chem B 2006;110(17):8535–9.
[26] Tang Z, Zhuang J, Wang X. Exfoliation of graphene from graphite and their self-assembly at the oil-water interface. Langmuir 2010;26(11):9045–9.
[27] Sutter P. Epitaxial graphene: how silicon leaves the scene. Nat Mater 2009;8(3):171–2.
[28] McArdle TJ, Chu JO, Zhu Y, Liu Z, Krishnan M, Breslin CM, et al. Multilayer epitaxial graphene formed by pyrolysis of polycrystalline silicon-carbide grown on c-plane sapphire substrates. Appl Phys Lett 2011;98:132108.
[29] Hussain F, Hojjati M, Okamoto M, Gorga RE. Review article: polymer–matrix nanocomposites, processing, manufacturing, and application: an overview. J Compos Mater 2006;40(17):1511–75.
[30] Sakhaee-Pour A. Elastic buckling of single-layered graphene sheet. Comput Mater Sci 2008;45(2):266–70.
[31] Belytschko T, Xiao SP, Schatz GC, Ruoff RS. Atomistic simulations of nanotube fracture. Phys Rev B 2002;65(23):235430.
[32] Li T-WC, Chou. A structural mechanics approach for the analysis of carbon nanotubes. Int J Solids Struct 2003;40(10):2487–99.
[33] Shokrieh MM, Rafiee R. On the tensile behavior of an embedded carbon nanotube in polymer matrix with non-bonded interphase region. Compos Struct 2010;92(3):647–52.
[34] Timoshenko S. Theory of plates and shells. London: McGraw-Hill Inc.; 1940.
[35] Scarpa F, Chowdhury R, Adhikari S. The transverse elasticity of bilayer graphene. Phys Lett A 2010;374(19):2053–7.
[36] Girifalco LA, Hodak M, Lee RS. Carbon nanotubes, buckyballs, ropes, and a universal graphitic potential. Phys Rev B 2000;62(19):13104–10.
[37] Battezzati L, Pisani C, Ricca F. Equilibrium conformation and surface motion of hydrocarbon molecules physisorbed on graphit. J Chem Soc, Faraday Trans 1975;71(2):1629–39.
[38] Dassault Systmes Simulia Corp., ABAQUS version 6.10 documentation and theory manual; 2011 <http://abaqus.civil.uwa.edu.au:2080/v6.10/index.html>.
[39] Yarrington P, Zhang J, Collier CS, Bednarcyk BA. Failure analysis of adhesively bonded composite joints. In: Proc of the 46th AIAA/ASME/ASCE/AHS/ASC structures, structural dynamics and materials conference, vol. 23; 2005.
[40] Hull D, Clyne TW. An introduction to compositematerials. Cambridge: Cambridge University Press; 1996.
[41] Georgantzinos S, Giannopoulos G, Katsareas D, Kakavas P, Anifantis N. Size-dependent non-linear mechanical properties of graphene nanoribbons. Comput Mater Sci 2011;50(7):20572062.
[42] Rafiee MA, Rafiee J, Srivastava I, Wang Z, Song H, Yu Z-Z, et al. Fracture and fatigue in graphene nanocomposites. Small 2010;6(2):179–83.
[43] Rafiee MA, Rafiee J, Wang Z, Song H, Yu Z-Z, Koratkar N. Enhanced mechanical properties of nanocomposites at low graphene. ACSNANO 2009;3(12):3884–90.
[44] Kim H, Abdala AA, Macosko CW. Graphene/polymer nanocomposites. ACSNANO 2009;43:6515–30.
[45] Liu XZQ, Fan X, Zhu C, Yao X, Liu Z. Mechanical and thermal properties of epoxy resin nanocomposites reinforced with graphene oxide. Polym-Plast Technol Eng 2012;51:251256.
[46] Li C, Browning AR, Christensen S, Strachan A. Atomistic simulations on multilayer graphene reinforced epoxy composites. Composites: Part A 2012;43:12931300.

[47] Cho J, Luo J, Daniel I. Mechanical characterization of graphite/epoxy nanocomposites by multi-scale analysis. Compos Sci Technol 2007;67:23992407.
[48] Ramanathan T, Abdala AA, Stankovich S, Dikin DA, Herrera-Alonso M, Piner RD, et al. Functionalized graphene sheets for polymer nanocomposites. Nat Nanotechnol 2008;3:327–31.
[49] Parashar A, Mertiny P. Representative volume element to estimate buckling behavior of graphene/polymer nanocomposite. Nanoscale Res Lett 2012;7:515.
[50] Montazeri A, Rafii-Tabar H. Multiscale modeling of graphene- and nanotube-based reinforced polymer nanocomposites. Phys Lett A 2011:4034–40.
[51] Tserpes KI, Papanikos P, Labeas G, Pantelakis SpG. Multi-scale modeling of tensile behavior of carbon nanotube-reinforced composites. Theor Appl Fract Mech 2008;49:51–60.
[52] Wernik JM, Meguid SA. Multiscale modeling of the nonlinear response of nano-reinforced polymers. Acta Mech 2011;217:1–16.
[53] Baykasoglu C, Mugan A. Coupled molecular/continuum mechanical modeling of graphene sheets. Physica E 2012;45:151–61.
[54] Baykasoglu C, Mugan A. Nonlinear fracture analysis of single-layer graphene sheets. Eng Fract Mech 2012;96:241–50.
[55] Tserpes KI, Papanikos P, Labeas G, Tsirkas SA. A progressive fracture model for carbon nanotubes. Composites: Part B 2006;37:662–9.
[56] Georgantzinos SK, Giannopoulos GI, Anifantis NK. Investigation of stressstrain behavior of single walled carbon nanotube/rubber composites by a multi-scale finite element method. Theor Appl Fract Mech 2009;52:158–64.
[57] Mohammadpour E, Awang M. Nonlinear finite-element modeling of graphene and single and multi-walled carbon nanotubes under axial tension. Appl Phys A 2012;106:581–8.
[58] Pei QX, Zhang YW, Shenoy VB. A molecular dynamics study of the mechanical properties of hydrogen functionalized graphene. Carbon 2010;48(3):898–904.